The pH Dependence of the 695 nm Charge Transfer Band Reveals the Population of an Intermediate State of the Alkaline Transition of Ferricytochrome *c* at Low Ion Concentrations[†]

Daniel Verbaro,[‡,§] Andrew Hagarman,[‡] Jonathan Soffer,[‡] and Reinhard Schweitzer-Stenner*,[‡]

Department of Chemistry and Department of Biology, Drexel University, 3141 Chestnut Street, Philadelphia, Pennsylvania 19104

Received December 2, 2008; Revised Manuscript Received February 17, 2009

ABSTRACT: We have measured and analyzed the pH dependence of the 695 nm charge transfer band of horse heart ferricytochrome *c* as a function of pH between 7.0 and 10.5 at high (50 mM) and low (0.5 mM) phosphate ion concentrations. Our data clearly reveal that the transition from the native state (III) to the two alkaline states (IV) involves two deprotonation steps which cannot be assigned to the two different lysine ligands associated with the two alkaline states. While the respective p*K* values are rather similar at high phosphate concentrations (9.23 and 9.14), they are clearly different at low anion concentrations (9.65 and 8.5). Apparently, the deprotonation that can be assigned to a p*K* of 8.5 populates an intermediate state termed III*, in which M80 is still an axial ligand. A comparison of Soret band CD spectra suggests that III* bears some similarity with the recently characterized thermally excited state III_h. Our data suggest that the current picture of the alkaline transition is incomplete. The obtained results might be of relevance for characterizing the structure of ferricytochrome *c* bound to anionic phospholipids.

Cytochrome *c* is a small heme protein in the intermembrane space of the mitochondria. It mediates the electron transfer from cytochrome *c* reductase to cytochrome *c* oxidase (*1, 2*), plays a pivotal role in apoptosis (*3*), and is also involved in the aggregation of α-synuclein, which is responsible for Parkinson's disease (*4*). Moreover, this protein has been used extensively as a model system for protein folding studies. The non-native states of cytochrome *c* play an important biological role in vivo (*1*−*3, 5*−*8*), so that the functional diversity reflects the conformational flexibility of the oxidized state. This relationship between structure and function led to a continuous interest in the transition of native ferri state III (populated at room temperature and neutral pH) to alkaline state IV, in which the M80 ligand of the heme is replaced with either K73 or K79 (*9*−*17*). The details of this reaction are still not fully understood.

Most investigations of the III → IV and other conformational transitions of the oxidized protein were carried out at high anion concentrations to maximize its stability (*10, 12, 15*−*17*). However, this complicates any meaningful thermodynamic analysis, because many anions bind to the positive patches on the protein surface (*18, 19*). This binding causes small structural changes which are nevertheless likely to be functionally relevant because they affect the Fe−M80 linkage between the heme and the flexible Ω-loop of the protein (*20*−*24*), which is a key determinant of the redox potential. Electrochemical studies of Sola and co-workers showed that the apparent p*K* value of the alkaline transition decreases with an increase in ionic strength (*13, 19*), but its dependence on anion binding has not yet been investigated in structural terms. Investigating the structure and dynamics of ferricytochrome *c* at low ionic strengths is of particular relevance due to the fact that it is necessary for, e.g., the complex formation with Apaf-1 and anionic lipids (*3, 8*).

The charge transfer band at 695 nm in the optical spectrum of ferricytochrome *c* has frequently been used for studying the III → IV transition, since it disappears in the alkaline state (*9*). Recently, we showed that this band can be subdivided into three sub-bands that can be assigned to subconformations of the Fe^{3+}−M80 linkage (*24*−*26*). Moreover, we found that the binding of $H_2PO_4^-$ ions at pH 6 causes a rather dramatic increase in the oscillator strength of the bands (*24*). We interpreted this as being indicative of a strengthening of the functionally pivotal Fe^{3+}−M80 linkage due to anion binding to the positively charged patch of cytochrome *c*. In this study, we measured the absorption and CD (circular dichroism) profile of the 695 nm band as a function of pH between 7.0 and 10.5 at high (50 mM phosphate buffer) and low (0.5 mM phosphate buffer) phosphate ion concentrations. The study, which was guided by the desire to study (a) the involvement of these substates in and (b) the influence of anion binding on the alkaline transition, yielded results which suggest that the current understanding of the alkaline transition has to be revised.

MATERIALS AND METHODS

Preparation of the Solution. Horse heart cytochrome *c* was purchased from Sigma-Aldrich Co. (St. Louis, MO) without

[†] D.V. was the recipient of a Maryanoff fellowship for summer research in Drexel's Chemistry Department.

* To whom correspondence should be addressed. Phone: (215) 895-2268. Fax: (215) 895-1265. E-mail: rschweitzer-stenner@drexel.edu.

[‡] Department of Chemistry.

[§] Department of Biology.

10.1021/bi802208f CCC: $40.75
Published on Web 02/17/2009

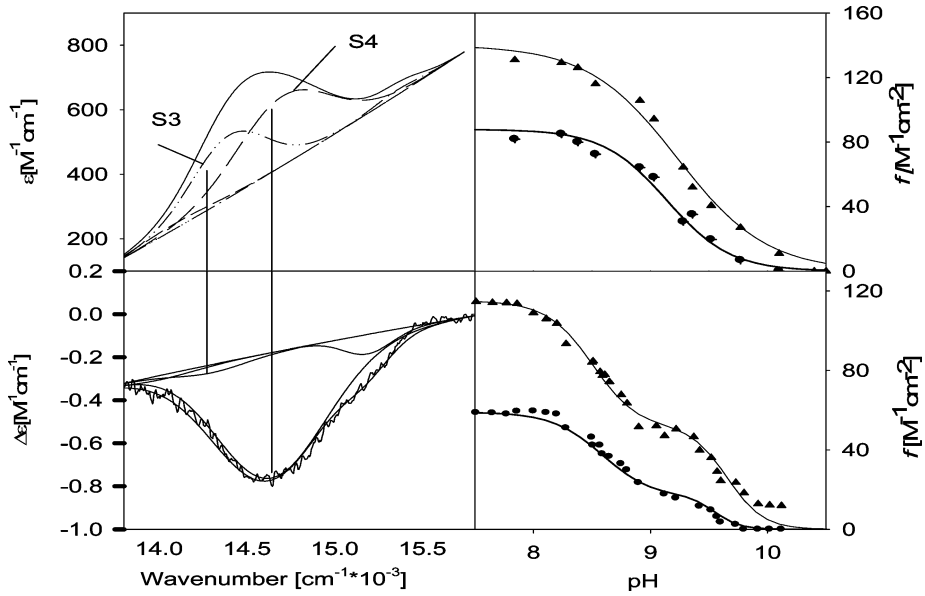

FIGURE 1: Absorption and CD band profiles (left column) of the 695 nm band of horse heart ferricytochrome *c* measured at pH 7 with a 50 mM phosphate buffer. The profiles were decomposed with a procedure described in Materials and Methods. Integrated (absorption) intensities (right column) of sub-bands S3 (●) and S4 (▲) as a function of pH measured with 50 mM (top panel) and 0.5 mM phosphate buffer (bottom panel).

further purification and dissolved in 0.5 mM (low phosphate ion concentration) and 50 mM potassium phosphate buffer (high phosphate ion concentration). A protein concentration of 5 mM was used for measurements of the 695 nm band region. Selected absorption and CD spectra of the B-band region were recorded with a protein concentration of 0.05 mM for both buffer concentrations. A small amount of potassium ferricyanide was added to each sample before proceeding to ensure complete oxidation.

Spectroscopy. A Jasco J-810 spectropolarimeter purged with N_2 was used to obtain the charge transfer (CT) and Soret band CD spectra. The CT band was recorded between 650 and 740 nm using a 10 mm quartz cell (Helma) with a data pitch of 0.2 nm, a continuous scanning speed of 50 nm/min, a response time of 1 s, and a bandwidth of 2.5 nm. A total of five accumulations for each pH were averaged at 20 °C. The Soret band region was measured between 350 and 550 nm using a 1 mm quartz cell with a data pitch of 0.1 nm, a continuous scanning speed of 500 nm/min, a response time of 1 s, and a bandwidth of 2.5 nm. A total of five accumulations for each pH were averaged at 20 °C. FTIR spectra of the highly concentrated sample (i.e., 5 mM) in a 0.5 mM $H_2PO_4^-$ buffer were recorded using a Biotools Chiral IR spectrometer with a 20 μm CaF_2 cell and 50 scans with an 8 cm^{-1} resolution in the amide I′ region.

Titration of Cytochrome c. The sample cell was filled with 2 mL of the 5 mM cytochrome *c* solution. The pH was measured with a micro size glass combination electrode (Fisher Scientific) directly in the sample cell as a function of 1 μL aliquots of NaOH being added, which increased the pH by ~0.2. The accuracy of the pH determination was ±0.01 pH unit. Absorption and CD spectra were recorded after each titration step until the 695 nm band was no longer detectable. This titration required, at the most, only 30 μL of 0.1 M NaOH. The corresponding dilution effect was negligible. We also measured the spectrum with a much lower concentration (0.5 mM) at pH 9 and reproduced the band profile observed with the higher concentration used for this study (Figure S1 of the Supporting Information; some deviations between the two profiles are due to problems with the baseline corrections for the 0.5 mM measurement). This rules out aggregation as a cause for the observed results, in accordance with the results of earlier sedimentation measurements, which showed that horse heart cytochrome *c* is monomeric at millimolar concentrations, since aggregation is prevented by the positively charged lysine residues which constitute the docking site for cytochrome *c* oxidase (*27*). A similar check was performed at neutral pH (*26*).

Decomposition of Spectra. Before the spectra were processed for analysis, reference spectra were used for background subtraction. MULTIFIT (*28*) was used to decompose both the absorption and the CD band profile of the 695 nm band into sub-bands. In contrast to the strategy adopted in earlier studies (*24, 26*), we did not subtract a baseline prior to the spectral decomposition process, because we found the final result to be somewhat dependent on the selection of the baseline type offered by MULTIFIT. Instead, the original band profiles were fitted by superimposing a set of Gaussian sub-bands with a quadratic function to account for the baseline predominantly constituted by the low-energy wing of the Q-band. Self-consistency of our analysis was achieved by using the same spectral parameters for all absorption and CD spectra. The thus obtained half-widths of the sub-bands were 500 cm^{-1} for S2, 500 cm^{-1} for S3, and 540 cm^{-1} for S4, and the corresponding wavenumber positions were 14.02 $\times 10^3$, 14.40 $\times 10^3$, and 14.7 $\times 10^3$ cm^{-1}, respectively. The integrated intensities of the sub-bands obtained from the fits, which are measures of the oscillator strength (absorption) and rotational strength (CD), were plotted as a function of pH to construct the titration curves.

RESULTS AND DISCUSSION

We measured and analyzed the absorption and circular dichroism (CD) profile of the 695 nm band of horse heart ferricytochrome *c* between pH 7.0 and 10.5 in increments

of 0.2 by adopting the protocol described above. The bands were self-consistently analyzed by being decomposed into sub-bands, which have the same half-widths, bandshapes, and wavenumber positions in the respective absorption and CD spectra. To this end, we adopted a protocol which is slightly different from that used by Dragomir et al. (*25*), as described in Materials and Methods. Figure 1 (left column) shows the band profiles measured at pH 7.0 at high phosphate ion concentrations. We found that the band is dominated by two sub-bands with rather different rotational strengths, which correspond to sub-bands S3 and S4 of Dragomir et al. (*25*). Sub-band S2 is very weak and will not be assessed in this study. The sub-bands are assigned to charge transfer transitions in different conformational substates of the Fe^{3+}−M80 linkage for reasons detailed in earlier publications (*25, 29*). The intensity distribution is somewhat different from what Shah and Schweitzer-Stenner obtained with the same buffer concentration (*24*). This difference might in part be due to the different strategies of spectral decomposition but should be predominantly attributed to the different pH values at which the respective experiments were conducted. A pH dependence of the 695 nm band between 6 and 7 has recently been reported (*26*).

The right column of Figure 1 exhibits the integrated intensities:

$$f_j = \int \varepsilon_j(\hat{\nu})\, \mathrm{d}\hat{\nu} \tag{1}$$

of the sub-bands S3 and S4 as a function of pH. The pH dependences of the respective rotational strengths R_j

$$R_j = \int \Delta\varepsilon_j(\hat{\nu})\, \mathrm{d}\hat{\nu} \tag{2}$$

are shown in Figure 2. ε and $\Delta\varepsilon$ denote the wavenumber-dependent molar extinction and ellipticity coefficients, respectively, and f_j reflects the (apparent) oscillator and rotational strength of considered sub-band *j*.

The titration curves of ferricytochrome *c* in 50 mM phosphate buffer are clearly monophasic and could be easily fitted by a simple protonation model, which assumes one (effective) p*K* value and some cooperativity reflecting the Coulomb interactions between protonatable groups in the heme pocket. The respective equation reads

$$f_j(\mathrm{pH}) = f_j^{\mathrm{III}}\left[1 + \left(\frac{K}{[\mathrm{H_3O}]^+}\right)^n\right]^{-1} \tag{3}$$

where *K* is the dissociation constant of the protonation process and f_j^{III} is the integrated intensity of the *j*th substate of native conformation III. A similar equation can be formulated for R_j(pH). Cooperativity is reflected by Hill coefficient *n*. The fit of eq 3 to the *f*(pH) and *R*(pH) data obtained at high phosphate concentrations yielded p*K* values of 9.2 ± 0.1 and 9.1 ± 0.1 for S3 and S4, respectively. The corresponding Hill coefficients of 1.14 and 1.6, respectively, are significantly different. The p*K* values are close to what Blouin et al. observed under nearly the same experimental conditions (*14*). By linearizing the titration curve, these authors showed that two protonatable groups with slightly different p*K* values are involved in the III → IV transition. We utilized the same equation and also obtained two p*K* values, i.e., 9.3 and 8.8. Blouin et al. assigned the two p*K* values to the parallel transitions from III to isomers IV_a and IV_b. As shown in Figures 1 and 2, the titration curves obtained at low anion concentrations are clearly biphasic. This has not yet been observed. On the other hand, the pH dependence of the redox potential is still monophasic at low ionic strengths (*13*). One is tempted to explain the biphasic titration by invoking coexisting IV isomers in which K73 and K79 are coordinated to the heme iron (*11, 12*). The reaction scheme would thus read as

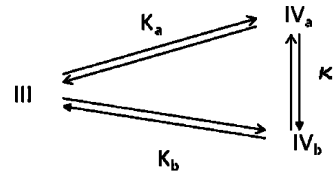

(R1)

The pH dependence of the sub-bands' intensities f_j thus reads as:

$$f_j(\mathrm{pH}) = f_j^{\mathrm{III}}\left\{1 + \left[\frac{K_a(1+\kappa)}{[\mathrm{H_3O}]^+}\right]^n\right\}^{-1} \tag{4}$$

where K_a and K_b are the dissociation constants for the protonation of IV_a and IV_b, respectively, and $\kappa = [IV_a]/[IV_b]$ is the equilibrium constant for the $IV_a \leftrightarrow IV_b$ isomerization. Note that K_b is substituted in eq 4 with $K_a\kappa$ to reflect the conservation of Gibbs energy in a thermodynamic cycle. A formal derivation of eq 4 is given in the Supporting Information. The thus described titration is not biphasic and can therefore not explain the biphasic behavior of *f*(pH). As a matter of fact, the model cannot explain the two similar but distinguishable p*K* values derived from the titration at high anion concentrations either. We invoked an alternative model which assumes two protonatable sites for each isomer. This scheme involves four different protonation states, but if $pK_1 \gg pK_2$, only a single intermediate (with one proton bound) will be substantially populated. We call this intermediate, for which the 695 nm band still exists, III*. The reaction scheme reads as

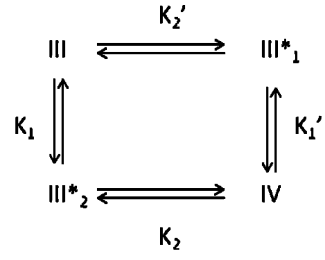

(R2)

where K_1, K_1', K_2, and K_2' denote the equilibrium constants of the indicated conversions. In the absence of any evidence to the contrary, we assumed that the two considered protonation processes proceed independently, so that $K_1 = K_1'$ and $K_2 = K_2'$. Thus, the pH dependence of the absorption band intensities can be written as

$$f_j(\mathrm{pH}) = \frac{f_j^{\mathrm{III}}}{1 + \left(\frac{K_1}{[H_3O^+]}\right)^{n_1} + \left(\frac{K_2}{[H_3O^+]}\right)^{n_2} + \frac{{K_1}^{n_1}{K_2}^{n_2}}{[H_3O^+]^{n_1+n_2}}} + f_j^{\mathrm{III}*} \left[\frac{1}{1 + \left(\frac{K_1}{[H_3O^+]}\right)^{n_1} + \left(\frac{[H_3O^+]^2}{K_2}\right)^{n_2} + \frac{{K_1}^{n_1}}{{K_2}^{n_2}}} + \frac{1}{1 + \left(\frac{K_2}{[H_3O^+]}\right)^{n_2} + \left(\frac{[H_3O^+]^2}{K_1}\right)^{n_1} + \frac{{K_2}^{n_2}}{{K_1}^{n_1}}}\right] \quad (5)$$

where $f_j^{\mathrm{III}*}$ is the intrinsic intensity of the intermediate. Equation 5 is based on the assumption that III_1* and III_2* exhibit the same *f* value, Of course, this is not necessarily the case, but as shown by our analysis, this minimal model I is sufficient to explain our data. The fit of eq 5 to the biphasic titration curves (Figures 1 and 2) yielded a pK_1 of 9.6 ± 0.1 and a pK_2 of 8.5 ± 0.1. for the S3 substate. The pK_1 value is slightly different for S4 (i.e., 9.54). The *f* values of the different protonation states are listed in Table 1. The respective p*K* values obtained from the fits to the four titration curves of S3 and S4 are identical within the limit of their statistical error. The titration curves for the rotational strength were analyzed as well by means of the same formalism; the results are also listed in Table 1. We used the obtained parameters to calculate the mole fractions χ_i (i = III, III_1*, III_2*, and IV). The result is depicted in Figure 3a. At neutral pH (7.0), nearly all proteins of the sample are in the III state ($\chi_{\mathrm{III}} = 0.99$), whereas state III_1* is predominant at pH 9.0 ($\chi_{\mathrm{III}_1*} = 0.91$). At pH 10, 91% of the proteins adopt alkaline state IV. For the sake of comparison, we used the two p*K* values inferred from the titrations performed with high anion concentrations (i.e., 8.8 and 9.3) to calculate the respective mole fractions of the protonation states. To this end, we used the Hill coefficient obtained from fits to the titrations obtained with high anion concentrations for n_1 and n_2. The results are displayed in Figure 3b. They reveal that states III and IV are still dominant at pH 7.5 and 10, respectively. Compared with the situation at low anion concentrations, intermediate state III_1* is now less populated at pH 9.0 (compared with the situation at low anion concentrations), and the respective mole fraction $\chi_{\mathrm{III}_1*} \approx 0.4$. The occupation of state III_2* is small ($\chi_{\mathrm{III}_2*} \approx 0.1$), but not negligible.

Table 1: Parameters Obtained from the Fits of the Titration Curves of the Indicated Sub-Bands of the Absorption (top part) and CD Band Profile (bottom part)[a]

band	pK_1	pK_2	f^{III} (M^{-1} cm^{-2})	$f^{\mathrm{III}*}$ (M^{-1} cm^{-2})	n_1	n_2
S3, 50 mM	9.2 ± 0.1		136	0	1.14	
S3, 0.5 mM	9.6 ± 0.1	8.5 ± 0.1	115	54.5	2.2	2.86
S4, 50 mM	9.1 ± 0.1		61	0	1.6	
S4, 0.5 mM	9.5 ± 0.1	8.6 ± 0.1	59	18.5	2	4

band	pK_1	pK_2	R^{III} (M^{-1} cm^{-2})	R^{III} (M^{-1} cm^{-2})	n_1	n_2
S3, 50 mM	9.2 ± 0.1		9	0	1.14	
S3, 0.5 mM	9.6 ± 0.1	8.5 ± 0.1	13	6.7	2.2	2.86
S4, 50 mM	9.1 ± 0.1		38	0	1.6	
S4, 0.5 mM	9.6 ± 0.1	8.6 ± 0.1	25	10.5	2	4

[a] The titration curves obtained for cytochrome *c* in 50 mM phosphate buffer were fitted with a model assuming the involvement of a single protonatable group, whereas the titration curves observed for cytochrome *c* in 0.5 mM phosphate buffer were fitted with a model assuming two protonatable groups, as outlined in the paper; f^{III} (R^{III}) and $f^{\mathrm{III}*}$ ($R^{\mathrm{III}*}$) are the oscillator (rotational) strengths associated with states III and III*, respectively. Hill coefficients (n_1 and n_2) were used to account for cooperativity.

It should be mentioned in this context that at least one p*K* (pK_2) should be considered as an apparent value which reflects two consecutive steps. As shown by Davis et al., kinetic measurements revealed a two-phase kinetics of the alkaline transition at high ion concentrations (*9*). The deprotonation occurs at a rather high pH (pK_{H} = 11.0) and is followed by a rather slow conformational transition to yield the final alkaline state. This second step gives rise to the much lower apparent p*K* value (9.0). It is obvious that the kinetic intermediate observed by Davis et al. cannot be identified with any of the III* states, because the conformational transition identified by their measurements is unimolecular and cannot be discriminated from the protonation step by equilibrium measurements.

Our results clearly reveal a two-step mechanism for the III → IV transitions. The first step involves the formation of state III*, for which the 695 nm band still depicts oscillator and rotational strength. If this band can be assigned to a S → Fe^{3+} charge transfer as suggested, our results indicate that

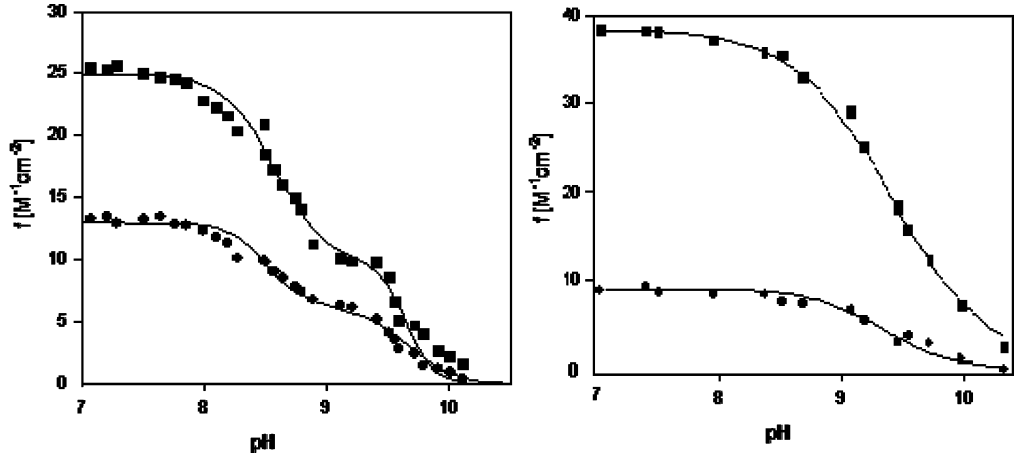

FIGURE 2: Rotational strength of the S3 (●) and S4 (■) sub-bands at 0.5 mM potassium phosphate (left) and 50 mM potassium phosphate (right). The solid lines were generated from the fit described in the paper.

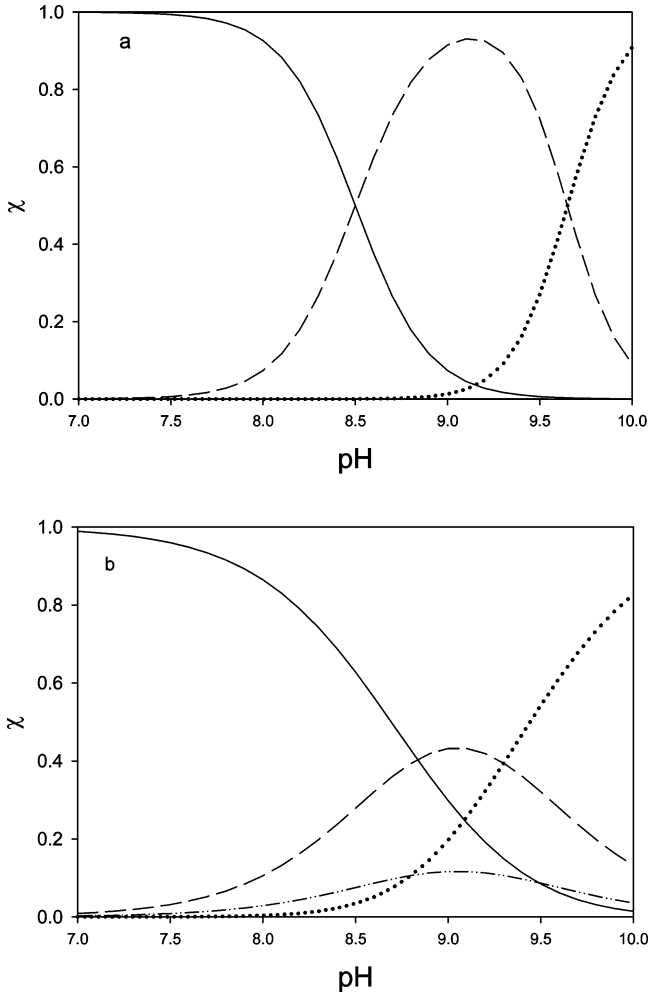

FIGURE 3: pH dependence of the mole fractions of the protonation states derived from an analysis of the titration curves in Figures 1 and 2 at (a) a low phosphate concentration and (b) a high phosphate concentration (state III, solid line; state III_1*, dashed line; state III_2*, dashed−dotted line; state IV, dotted line).

M80 is still coordinated to the heme iron, though the respective interaction energies are certainly weaker than those in III. This leads us to suppose that III* is very similar to though not identical with thermal intermediate III_h (*15*), which we recently showed to be different from state IV, contrary to claims in the literature. Figure 4a shows the visible CD spectra of the B-band taken at pH 8.0 (III), 9.0 (III*), and 10.0 (IV) at low ionic strengths. Not only is the state III* spectrum clearly distinct from that of state IV, it also closely resembles the CD spectrum of III_h reported by Hagarman et al. (*15*), in that it displays a symmetric couplet which is diagnostic of substantial B-band splitting by the internal electric field of the protein (*30*). This splitting is (nearly) absent in alkaline state IV. For the sake of comparison, we also measured the corresponding CD spectrum of the B-band region of the protein in the 50 mM phosphate buffer, which are shown in Figure 4b. At pH 8.0, the couplet appears upshifted (i.e., increase in the maximum at the expense of the minimum) compared with the respective CD signal in Figure 4a. This is in agreement with the CD spectra reported by Shah and Schweitzer-Stenner (*24*), which were taken at more acidic pH. At pH 10, the positive Cotton bands seem not to depend on the anion concentration. At pH 9, the spectrum obtained with high anion concentrations is only slightly different from that obtained at pH 8 and thus much more pronounced than the signal obtained at low anion concentrations, indicating that state III is even more populated at pH 9 than suggested by the somewhat hypothetical mole fractions displayed in Figure 3b.

One might suspect that protein aggregation might become involved at the chosen low anion concentration, because of the high protein concentration, which exceeds the molarity of the buffer. As mentioned in Materials and Methods, the similarity of 695 nm band profiles recorded with protein concentrations of 5 and 0.5 mM rules out this possibility (Figure S1 of the Supporting Information). The very fact that the band still exists in state III* also argues against aggregation, which has been shown to lead to its elimination (*31*). To be absolutely sure about this issue, we measured the amide I′ FTIR spectrum of the 5 mM sample under low-ionic strength buffer conditions. The FTIR spectra from 1600 to 1700 cm^{-1} (amide I′ region) are characteristic of an α-helix, with a single band centered at 1650 cm^{-1}, and no indication of aggregation (Figure S2 of the Supporting Information).

Recently, a structural model of one of the alkaline states (M80 → K73) has emerged from a very detailed NMR study by Assfalg et al. (*16*). The investigation was carried out at pH 11, which ensures the population of state IV and to some extent even state V (*12*). The results revealed that the proximal side of the heme cavity, which contains axial ligand H18, remains intact. Structural changes involve predominantly the 70−80 loop and the 50s helix. This result implies that the electronically induced splitting of the Soret band probed by its CD spectrum is produced by charges in the flexible distal loop of the protein. The intermediate state still exhibits this splitting and distinguishes itself from state III only by a more symmetric couplet, which could reflect a reorientation of amino acid residues in the 70−80s loop rather than the structural changes observed for state IV (*16*). Hagarman et al. suggested F82 as a very likely candidate (*15*), based on its established influence on the CD couplet of the Soret band (*32*).

Our results suggest the necessity to revise the current picture of the III → IV transition. The two deprotonation processes recently assigned to III → IV_a and III → IV_b transitions in a parallel reaction scheme must instead be understood as reflecting two consecutive reactions, i.e., the population of an III_h-like intermediate and the subsequent transition into either IV_a or IV_b. Anion (phosphate ion) binding increases the pK value of the III → III* transition, whereas the opposite is the case for the III* → IV transitions. A comparison with the electrochemical data reported by the Sola group (*13, 19*) suggests that it is the III → III* transition which actually causes the decrease in the redox potential at alkaline pH. The Hill coefficients of the two transitions are apparently much smaller than those obtained from the two-state analysis of the titration at high phosphate ion concentrations. Since the exact mechanism underlying the cooperativity of proton binding is not yet understood, one can only speculate about the reasons for the lower cooperativity at low ion concentrations. X-ray scattering studies have shown that the protein is less compact at low ionic strengths (*33*), so that the interaction energy between proton binding sites becomes smaller, thus reducing cooperativity.

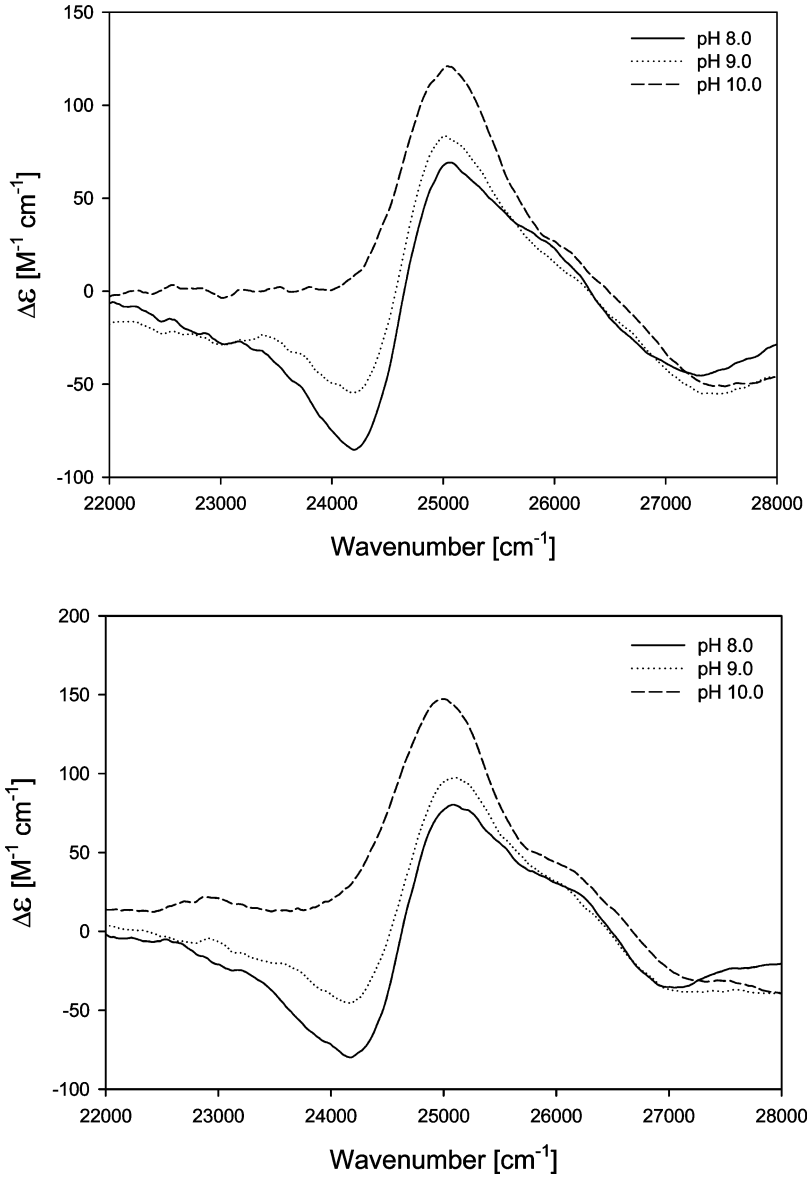

FIGURE 4: CD spectra of the Soret band region of ferricytochrome *c* recorded at pH 8.0 (solid line), 9.0 (dotted line), and 10.0 (dashed line) at low (a) and high (b) ionic strengths.

It has to be mentioned in this context that the existence of a thermodynamic intermediate of the III → IV transition of horse heart cytochrome *c* has recently been reported by Weinkam et al. (*17*). These authors used a very elegant technique, i.e., the selected deuteration of side chains in combination with FTIR spectroscopy, to probe structural changes involved in the alkaline transition. The experiments were conducted at high phosphate (50 mM) and sodium chloride (200 mM) concentrations, so that their results are not directly comparable with those of our study. Their results led them to subdivide the alkaline transition into two steps with midpoints at pH 8.8 and 10.2. They attributed the former to a transition from state III to an intermediate designated as state 3.5, whereas the second step was assigned to the formation of state(s) IV. The III → 3.5 transition was found to involve only conformational changes of the M80 ligand, but not any of the lysine ligands. There are several differences between their results and ours. Weinkam et al. claim that the III → 3.5 transition leads to a complete disappearance of the 695 nm band, which can therefore not be interpreted as reflecting a loss of the Fe−M80 coordination, which they thought still existed in 3.5. Intermediate state III* inferred from our data still exhibits considerable 695 nm band intensity and rotational strength. Moreover, the Weinkam et al. study did not explicitly consider the finding of Blouin et al. (*14*), who showed that the monophasic titration curve of the 695 nm band observed at high phosphate ion concentrations can still be decomposed into two protonation steps, which we could now clearly resolve at low anion concentrations. This indicates that state III_1* also becomes populated with high anion concentrations, though in a very small pH range and to a much lesser extent than observed at low anion concentrations (cf. Figure 3b). We therefore conclude that state 3.5 reported by Weinkam et al. is not identical with state III_1* inferred from our study. However, we wonder whether 3.5 could be identified with state III_2*, which, as argued above, can become populated at high anion concentrations.

We wonder about the possibility that state III* is involved in a conformational transition caused by the binding of cytochrome *c* to anionic phospholipids. Belikova et al. used the 695 nm band to probe structural changes caused by

interactions between the protein- and cardiolipin-containing liposomes and found the intensity of the band to be substantially reduced at low ionic strengths (*8*). They interpreted this as reflecting a protein fraction for which the ligand (M80) has been lost. This misligation would be a IV-like conformation. Our results reveal the possibility that the liposome−protein interaction actually stabilizes state III*. Experiments for testing this hypothesis are underway in our laboratory. Antalík et al. reported an increase in the 695 nm band upon the binding of polyglutamate to horse heart ferricytochrome *c* in a 2 mM phosphate buffer (*34*). This would be in line with results of Shah and Schweitzer-Stenner, who showed that an occupation of anion binding sites yields an increase in the 695 nm oscillator strength (*24*). However, a comparison of the spectra reveals that hydrogen phosphate ions are much more effective in this regard.

SUPPORTING INFORMATION AVAILABLE

Derivation of eq 4, Figure S1, and Figure S2. This material is available free of charge via the Internet at http://pubs.acs.org.

REFERENCES

1. Weber, C., Michel, B., and Bosshard, H. R. (1987) Spectroscopic Analysis of the Cytochrome c Oxidase-Cytochrome c Complexes: Circular Dichroism and Magnetic Circular Dichroism Measurements Reveal Changes of Cytochrome c Heme Geometry Imposed by Complex Formation. *Proc. Natl. Acad. Sci. U.S.A. 84*, 6687–6691.
2. Garber, E. A. E., and Margoliash, E. (1994) Circular dichroism studies of the binding of mammalian and non-mammalian cytochromes c to cytochrome c oxidase, cytochrome c peroxidase, and polyanions. *Biochim. Biophys. Acta 1187*, 289–295.
3. Purring-Koch, C., and McLendon, G. (2000) Cytochrome c binding to Apaf-1: The effects of dAtp and ionic strength. *Proc. Natl. Acad. Sci. U.S.A. 97*, 11928–11931.
4. Ruf, R. A. S., Lutz, E. A., Zigoneanu, I. G., and Pielak, G. J. (2008) α-Synuclein Conformation Affects Its Tyrosine-Dependent Oxidation Aggregation. *Biochemistry 47*, 13604–13609.
5. Pinheiro, T. J. T., Elöve, G., Watts, A., and Roder, H. (1997) Structural and Kinetic Description of Cytochrome c Unfolding Induced by the Interaction with Lipid Vesicles. *Biochemistry 36*, 13122–13132.
6. Cortese, J. D., Voglino, A. L., and Hackenbrock, C. R. (1998) Multiple Conformations of Physiological Membrane-Bound Cytochrome c. *Biochemistry 37*, 6402–6409.
7. Berezhna, S., Wohlrab, H., and Champion, P. M. (2003) Resonance Raman Investigations of Cytochrome c Conformational Change upon Interaction with the Membranes of Intact and Ca^{2+}-Exposed Mitochondria. *Biochemistry 42*, 6149–6158.
8. Belikova, N. A., Vladimirov, Y. A., Osipov, A. N., Kapralov, A. A., Tyurin, V. A., Potapovich, M. V., Basova, L. V., Peterson, J., Kurnikov, I. V., and Kagan, V. E. (2006) Peroxidase activity and structural transitions of cytochrome c bound to cardiolipin-containing membranes. *Biochemistry 45*, 4998–5009.
9. Davis, L. A., Schejter, A., and Hess, G. P. (1973) Alkaline Isomerization of oxidized cytochrome c. *J. Biol. Chem. 249*, 2624–2632.
10. Barker, P. D., and Mauk, A. G. (1992) pH-linked conformational regulation of a metalloprotein oxidation-reduction equilibrium: Electrochemical analysis of the alkaline form of cytochrome c. *J. Am. Chem. Soc. 114*, 3619–3624.
11. Rossel, F. I., Ferrer, J. C., and Mauk, A. G. (1998) Proton-linked protein conformational switching: Definition of the alkaline conformational transition of yeast iso-l-ferricytochrome c. *J. Am. Chem. Soc. 120*, 11234–11245.
12. Döpner, S., Hildebrandt, P., Rosell, F. I., and Mauk, A. G. (1998) The alkaline conformational transitions of ferricytochrome c studied by resonance Raman spectroscopy. *J. Am. Chem. Soc. 120*, 11246–11255.
13. Battistuzzi, G., Borsari, M., Loschi, L., Martinelli, A., and Sola, M. (1999) Thermodynamics of the alkaline transition of cytochrome c. *Biochemistry 38*, 7900–7907.
14. Blouin, C., Guillemette, J. G., and Wallace, C. J. A. (2001) Resolving the individual components of a pH-induced conformational change. *Biophys. J. 81*, 2331–2338.
15. Hagarman, A., Duitch, L., and Schweitzer-Stenner, R. (2008) The Conformational Manifold of Ferricytochromec Explored by Visible and Far-UV Electronic Circular Dichroism Spectroscopy. *Biochemistry 47*, 9667–9677.
16. Assfalg, M., Bertini, I., Dolfi, A., Turano, P., Mauk, A. G., Rossel, F. I., and Gray, H. B. (2003) Structural Model for an Alkaline Form of Ferricytochrome c. *J. Am. Chem. Soc. 125*, 2913–2922.
17. Weinkam, P., Zimmermann, J., Sagle, L. B., Matsuda, S., Dawson, P. E., Wolynes, P. G., and Romesberg, F. E. (2008) Cahracterization of Alkaline Transitions in Ferricytochrome c Using Carbon−Deuterium Infrared Probes. *Biochemistry 47*, 13470–13480.
18. Battistuzzi, G., Loschi, L., Borsari, M., and Sola, M. (1999) Effects of nonspecific ion-protein interactions on the redox chemistry of cytochrome c. *JBIC, J. Biol. Inorg. Chem. 4*, 601–607.
19. Battistuzzi, G., Borsari, M., and Sola, M. (2001) Medium and Temperature Effects on the Redox Chemistry of Cytochrome c. *Eur. J. Inorg. Chem.,* 2989–3004.
20. Feng, Y., and Englander, S. W. (1990) Salt dependent Structural Change and Ion Binding in Cytochromec Studied by Two-Dimensional Proton NMR. *Biochemistry 29*, 3505–3509.
21. Banci, L., Bertini, I., Redding, T., and Turano, P. (1998) Monitoring the conformational flexibility of cytochrome c at low ionic strength by H-NMR spectroscopy. *Eur. J. Biochem. 1998*, 271–278.
22. Sanishvili, R., Volz, K. W., Westbrook, E. M., and Margoliash, E. (1995) The low ionic strength crystal structure of horse cytochrome c at 2.1 Å resolution and comparison with the high ionic strength counterpart. *Structure 3*, 707–716.
23. Moench, S. J., Shi, T.-M., and Satterlee, J. S. (1991) Proton-NMR studies of the effects of ionic strength and pH on the hyperfine-shifted resonances and phenylalanine-82 environment of three species of mitochondrial ferricytochrome c. *Eur. J. Biochem. 197*, 631–641.
24. Shah, R., and Schweitzer-Stenner, R. (2008) Structural changes of horse heart ferricytochrome c induced by changes of ionic strength and anion binding. *Biochemistry 47*, 5250–5257.
25. Dragomir, I., Hagarman, A., Wallace, C., and Schweitzer-Stenner, R. (2007) Optical band splitting and electronic perturbations of the heme chromophore in cytochrome c at room temperature probed by visible electronic circular dichroism spectroscopy. *Biophys. J. 92*, 989–998.
26. Schweitzer-Stenner, R., Shah, R., Hagarman, A., and Dragomir, I. (2007) Conformational substates of horse heart cytochrome c exhibit different thermal unfolding of the heme cavity. *J. Phys. Chem. B 111*, 9057–9061.
27. Whitford, D., Concar, D. W., and Williams, R. J. P. (2001) The promotion of self-association of horse-heart cytochrome c by hexametaphosphate anions. *Eur. J. Biochem. 199*, 561–568.
28. Jentzen, W., Unger, E., Karvounis, G., Shelnutt, J. A., Dreybrodt, W., and Schweitzer-Stenner, R. (1996) Conformational Properties of Nickel(II) Octaethylporphyrin in Solution. 1. Resonance Excitation Profiles and Temperature Dependence of Structure-Sensitive Raman Lines. *J. Phys. Chem. 100*, 14184–14191.
29. Schweitzer-Stenner, R., Gorden, J. P., and Hagarman, A. (2007) The asymmetric band profile of the Soret band of deoxymyoglobin is caused by electronic and vibronic perturbations of the heme group rather than by a doming deformation. *J. Chem. Phys. 127*, 135103.
30. Schweitzer-Stenner, R. (2008) The Internal Electric Field in Cytochrome c Explored by Visible Electronic Circular Dichroism Spectroscopy. *J. Phys. Chem. B 112*, 10358–10366.
31. Filosa, A., and English, A. M. (2000) Probing local thermal stabilities of bovine, horse, and tuna ferricytochromes c at pH 7. *JBIC, J. Biol. Inorg. Chem. 4*, 448–454.
32. Pielak, G. J., Oikawa, K., Mauk, A. G., Smith, M., and Kay, C. M. (1986) Elimination of the Negative Soret Cotton Effect of Cytochrome c by Replacement of the Invariant Phenylalanine Using Site-Directed Mutagenesis. *J. Am. Chem. Soc. 108*, 2724–2727.
33. Trewhella, J., Carlson, V. A. P., Curtis, E. H., and Heidorn, D. B. (1988) Differences in the solution structures of oxidized and reduced cytochrome c measured by small-angle X-ray scattering. *Biochemistry 27*, 1121–1125.
34. Antalík, M., Bágelòvá, J., Gažová, Z., Musatov, A., and Fedunová, D. (2003) Effect of varying polyglutamate chain length on the structure and stability of ferricytochrome c. *Biochim. Biophys. Acta 1646*, 11.

BI802208F